Fuel 235 (2019) 515–521

Contents lists available at ScienceDirect

Fuel

journal homepage: www.elsevier.com/locate/fuel

Ethanol oxidation with high water content: A reactive molecular dynamics simulation study

Muye Feng, Xi Zhuo Jiang, Weilin Zeng, Kai H. Luo*, Paul Hellier

Department of Mechanical Engineering, University College London, Torrington Place, London WC1E 7JE, UK

ARTICLE INFO

Keywords:
Ethanol oxidation
Water
Molecular dynamics simulation
Reactive force field

ABSTRACT

Ethanol is a potential alternative to conventional fossil fuels. However, the required dewatering process to produce anhydrous ethanol is extremely energy-intensive and expensive. A promising solution is the direct use of hydrous ethanol for combustion applications, which can dramatically reduce the production cost. Many researchers have undertaken experiments demonstrating the feasibility and advantages of burning hydrous ethanol solely as a fuel. In this study, molecular dynamics (MD) simulation with the reactive force field (ReaxFF) is employed to investigate the fundamental reaction mechanisms of hydrous ethanol oxidation in comparison with the ethanol oxidation under fuel-air condition in order to understand the effects of water addition on ethanol oxidation. The results show that the reaction rate of ethanol oxidation is faster in water than in nitrogen environment and the presence of water advances the ionisation process and accelerates the radical production rate thereby enhancing the oxidation reaction. Additionally, it is suggested that the water content plays a vital role in reactions at low temperatures but that effect can be ignored at high temperatures. The detailed reaction pathways and time evolution of relevant key species indicate that H_2O promotes many reactions involving OH generation and these OH radicals also facilitate its reactions with C_1 & C_2 intermediates as well as the dehydrogenation of C_1 & C_2 intermediates. Similarly, CO production is reduced in hydrous ethanol oxidation as a result of CO reaction with OH converting the CO to CO_2 ultimately. Therefore, it is the addition of water that promotes the OH production due to the chemical effect of H_2O leading to the enhancement of ethanol oxidation and reduction of CO production. In summary, this research provides the scientific base for the direct use of hydrous ethanol as a fuel for combustion systems with a low cost.

1. Introduction

The finite resources of conventional fossil fuels and the severe problem of combustion emissions have prompted the development of environmentally-friendly alternative fuels. Ethanol, as a widely acknowledged renewable resource has numerous advantages. When ethanol is used as a fuel additive in internal combustion (IC) engines, it can suppress soot formation and reduce pollutant emissions [1]. Moreover, the high knock resistance of ethanol can increase the overall octane rating of blends of ethanol and fossil gasoline, potentially permitting spark ignition (SI) engine operation at higher compression ratios and thus thermal efficiencies [2]. However, ethanol derived from biomass has inherent high water content, and the distillation and dehydration processes needed to obtain anhydrous ethanol are both energy-intensive [3]. Data shows that the energy required for ethanol distillation grows exponentially as the fraction volume of ethanol increases and 37% of the total production cost is spent on dewatering activities [4]. Therefore, it is of great interest to study oxidation of hydrous ethanol with high water concentration, as this could dramatically save energy and cost during production by enabling the direct use of hydrous ethanol.

Hydrous ethanol oxidation has been studied for a long time by both experiments and simulations. Rahman et al. [5] investigated the combustion characteristics of wet ethanol by laser ignition. They found that the combustion rate was accelerated with the addition of water in ethanol and the laser ignition delay was shorter compared to the anhydrous ethanol. Their simulation also demonstrated that the adiabatic flame temperature and laminar burning velocity were reduced as a result of the water blending. The phenomenon of laminar burning velocity decrease was also observed in Liang et al.'s experiment and numerical modelling [6]. Breaux and Acharya studied the effect of water addition on swirl-stabilized ethanol/air flames and concluded that the exhaust temperature was decreased leading to the reduction of nitrogen oxides emissions [7]. A homogeneous charge compression ignition

* Corresponding author.
E-mail address: k.luo@ucl.ac.uk (K.H. Luo).

https://doi.org/10.1016/j.fuel.2018.08.040
Received 11 February 2018; Received in revised form 6 August 2018; Accepted 9 August 2018

(HCCI) engine retrofitted with an exhaust heat recovery system was developed by Saxena et al. and they explored the direct use of wet ethanol as the fuel [8]. The results showed that the best operating conditions for the engine could be achieved by burning hydrous ethanol. Similar outcomes for the usage of wet ethanol in an HCCI engine were obtained by Mack et al. [9]. Munsin et al. tested the performance and emissions of a SI engine fuelled with hydrous ethanol and reported that both regulated and unregulated emissions could be reduced if a catalytic converter is provided [10]. To sum up, it was suggested that direct oxidation of hydrous ethanol could be more efficient [11] and cost-effective [12] than dehydrated ethanol in many combustion applications, including IC engines. On the other hand, burning hydrous ethanol reduces the fuel calorific value, and the presence of water blended with ethanol has seen increased specific fuel consumption in engine experiments, and can result in higher NO_x emissions if ignition timing is advanced in order to take advantage of enhanced knock resistance and produce higher power output [13]. In tests of hydrous ethanol in a SI engine at constant load and speed, with an increase in water content from 20% to 40%, Munsin et al. [10] observed increases in engine-out emissions of formaldehyde and acetaldehyde in addition to CO and HC. Furthermore, the use of hydrous ethanol in blends with fossil gasoline can result in phase separation, compromising the stability and storage potential of the fuel blend [14].

Previous experiments and simulations have proved hydrous ethanol to be a promising alternative fuel, but the underlying mechanisms of hydrous ethanol oxidation are still poorly understood. Molecular Dynamics (MD) simulation with the Reactive Force Field (ReaxFF) is an efficient method to study oxidation reactions at the atomic level and it is becoming increasingly popular due to its feasibility for large scale reactive systems. Quantum Mechanics (QM) methods are able to produce extremely accurate results, but it is computationally very expensive or impossible to study the full dynamics of large reactive systems. Empirical Force Field methods are applicable for large scale simulations with acceptable computational resources but they usually cannot describe chemical reactions. The ReaxFF method is capable of modelling dissociation, transition and formation of bonds for chemical reactions based on the bond order concept, which helps to bridge the gap between QM and classical MD methods [15]. A high level of accuracy can be obtained even when conducting a large reactive simulation for a long time and it is much more computationally cost-efficient than QM methods. More details of the ReaxFF formulation and development can be found in [15–18]. On the other hand, MD or ReaxFF MD has its limitations. The principal limiting factor is the high computational cost of classical MD and especially ReaxFF MD, which sets a practical limitation on the size of the simulated system (to typically several millions of atoms at present [18]). This also sets a limit on the physical time that can be simulated up to microseconds. Therefore, classical/ReaxFF MD is best suited for fundamental studies of small and fast-changing systems, where the unknown mechanisms are dominated by molecular interactions. Such limitations have been significantly lifted in the past few decades, thanks to the rapid advancement in computing hardware and software. This trend is set to continue as the exascale computing era is fast approaching.

In this study, ReaxFF MD simulations are performed to investigate the fundamental reaction mechanisms of hydrous ethanol oxidation in comparison with ethanol oxidation under fuel-air conditions. By analysing the time evolution of the reaction and the atomic trajectory, the reaction rates and detailed reaction pathways are achieved. Finally, the effects of water addition on ethanol oxidation are revealed.

2. Computational methods

All the MD simulations are performed using the ReaxFF formulation implemented in LAMMPS (Large-scale Atomic/Molecular Massively Parallel Simulator) package [19,20], with a ReaxFF force field of C/H/O/N parameters [21]. Three 3-dimensional systems with different gas phase components and cubic simulation boxes are built at the same density of 0.062 g/cm^3. The periodic boundary condition is applied in all three directions. The details of the reactive systems studied are shown in Table 1. The stoichiometric condition of ethanol and oxygen (1:3) is adopted in all the three systems. System 1 is chosen to represent the fuel-air oxidation environment. (In the air, the proportion of oxygen and nitrogen molecules is approximately 1:4, which is calculated based on their volume fractions and the total density.) It is worth noting that nitrogen reaction is not observed within the studied time scale of ReaxFF MD simulations. Hence, Systems 2 and 3 are simplified with no nitrogen molecules from the perspective of setting up and running the simulations. To study the effects of high water concentration, the 480 nitrogen molecules are simply replaced with 480 water molecules in System 2. For System 3, the number of water molecules is reduced to 20 in order to investigate the ethanol oxidation with different ethanol/water ratios. The size of the cubic simulation boxes is adjusted accordingly to keep the same density for all the three systems.

Table 1
Construction details of the studied systems.

System	No. of Molecules				Size (Å)
	C_2H_6O	O_2	H_2O	N_2	
1	40	120	0	480	80.00
2	40	120	480	0	72.65
3	40	120	20	0	54.48

The canonical ensemble (NVT) is used for all the MD simulations in conjunction with the Nosé-Hoover thermostat employing a damping constant of 100 fs. Before the reactive simulation, every system undergoes energy minimization using the conjugate gradient algorithm to optimize the initial geometric configuration, followed by the NVT equilibration at 1000 K for 50 ps. After the equilibrium, a series of reactive NVT MD simulations for each system are performed for 1000 ps at temperatures ranging from 2000 K to 3000 K with an increment of 200 K. In previous ReaxFF MD simulations, particularly for combustion, employing a high temperature to accelerate the reactions is a common strategy to overcome the limitation of computing power [16,22–32]. More importantly, the present research is a comparative study of different cases, so the absolute temperature used is less important. A time step of 0.1 fs, which was found suitable for high-temperature (2500 K) ReaxFF MD simulations [16], is adopted for both the equilibrating and reactive simulations. The bonding information and dynamic trajectory are recorded every 100 fs. For species analysis, a 0.2 bond order cutoff is chosen to recognize the molecules forming during the simulation because a low cutoff value is helpful for capturing all the reactions involving those with very short-lived species [16]. Every case (one system at one temperature) has three parallel simulations set up to be averaged for further analysis and each of them has a unique starting configuration. Therefore, totally 54 simulations are carried out. The reaction pathways are analysed by Chemical Trajectory AnalYzer (ChemTraYzer) scripts [27]. All the visualisations of simulation results are generated using Visual Molecular Dynamics (VMD) software [33].

3. Results and discussions

3.1. Time evolution of potential energy

Fig. 1 describes the time evolution of potential energy for ethanol oxidation in both O_2/N_2 and O_2/H_2O atmospheres at various temperatures from 2000 K to 3000 K. Overall, the potential energy firstly rises to a peak point and then drops down as the time passes. However, higher temperature leads to more rapid increasing and decreasing of the potential energy, which means that the heat absorption and release are accelerated so that the ethanol oxidation is promoted by the elevated temperature. The comparison of Fig. 1a and 1b clearly shows that the

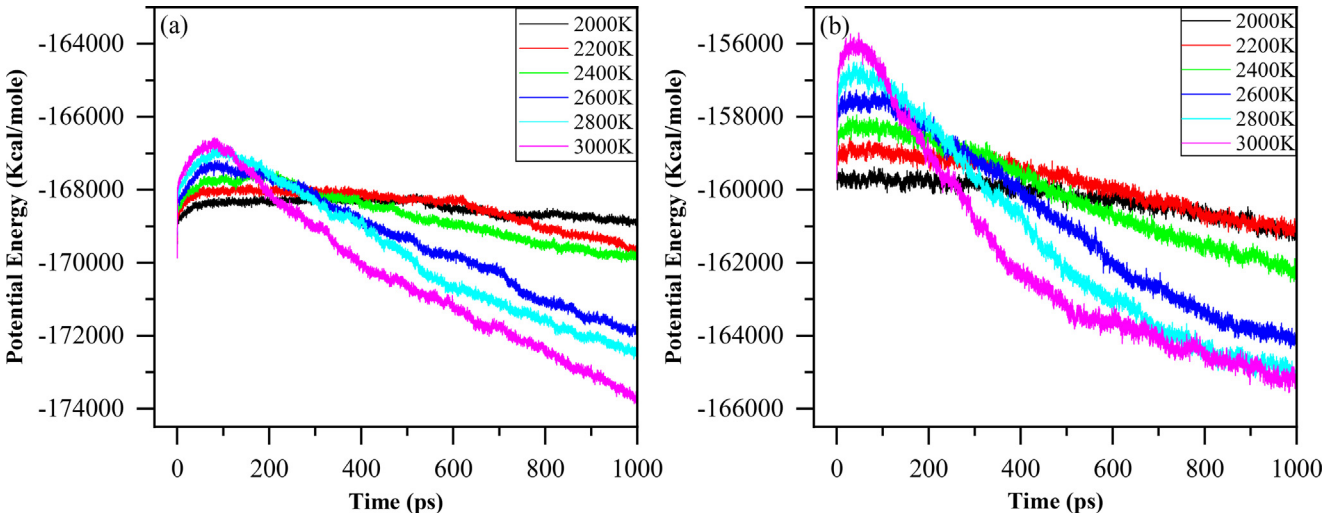

Fig. 1. Time evolution of potential energy during NVT MD simulations of ethanol oxidation from 2000 K to 3000 K in (a) O_2/N_2 and (b) O_2/H_2O environments.

amount of the absorbed energy (potential energy difference between the starting point and the maximum point) at the initial stage of the reaction is much more in O_2/H_2O than in O_2/N_2 environment, as is the amount of the heat release (potential energy difference between the maximum point and the end point) at a later stage. Likewise, the processes of heat absorption and release are faster in H_2O environment. These results imply that water does participate in and facilitate the reaction of ethanol oxidation.

3.2. Reaction rate under various conditions

The time evolution of the number of ethanol molecules over a temperature range from 2000 K to 3000 K for all three systems is used to investigate the reaction rate under various conditions. Fig. 2 shows the results of ethanol oxidation in N_2 and H_2O environments. The reaction rate of ethanol increases remarkably as temperatures rise in both cases. In addition, the consumption of ethanol is faster in O_2/H_2O than in O_2/N_2 at all studied temperatures, which indicates that ethanol oxidation is enhanced by replacing N_2 with H_2O. This phenomenon of improved ethanol oxidation with water was also observed in a previous experiment [5]. From 2400 K, the reaction rate of ethanol in O_2/H_2O is

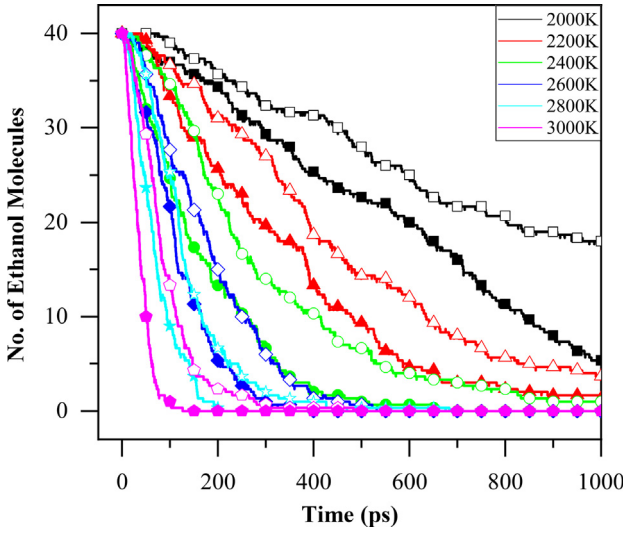

Fig. 2. Time evolution of ethanol molecule number during NVT MD simulations of ethanol oxidation from 2000 K to 3000 K in O_2/N_2 (hollow symbol) and O_2/H_2O (solid symbol) environments.

almost the same and even slightly higher than in O_2/N_2 at the next temperature point. This means that a similar reaction rate of ethanol in N_2 environment can be achieved at a 200 K lower temperature in H_2O environment when the temperature of ethanol oxidation in N_2 environment goes beyond 2600 K. The aforementioned results can also be supported by the time evolution of species number as illustrated in Fig. 3. Firstly, the peak value of species number is successively reached by a descending temperature order and the climbing rate is faster with the boosted temperature, which is consistent with the fact that higher temperature results in quicker reaction. Although there is not a significant difference in the maximum species number generated during the reactions at each temperature between ethanol oxidation in N_2 and H_2O environments, other distinctions are obvious. The time to reach the peak species number is shorter in O_2/H_2O than in O_2/N_2 at each temperature, which agrees with experimental results that the presence of water in ethanol advances the ionisation process and accelerates the radical production rate [5]. In addition, the rising and falling rates of the species number are more rapid in H_2O environment verifying the enhancement of ethanol oxidation with water compared to nitrogen.

The results of ethanol oxidation with two different ethanol/water ratios are depicted in Fig. 4. Generally, the reaction rate increases as the water content decreases, as would be expected. However, the difference in reaction rate between the two becomes smaller with increasing temperature. At 3000 K, the two lines nearly collapse into each other. This suggests that the water content of ethanol plays a vital role in the reaction rate at low temperatures but is significantly less important at high temperatures. Further studies are needed to determine whether a threshold of effect of water content on reaction rate exists under certain conditions.

3.3. Reaction pathways and time evolution of key species

All the simulation results from different temperatures and replicas are merged into one single mechanism to explore the reaction pathways of ethanol oxidation in N_2 and H_2O environments, respectively. The full list of elementary reactions (Table S1 in the supplementary material) is generated by filtering out the pathways with less than 40 accumulated total flux, resulting in 23 reactions for O_2/N_2 and 38 reactions for O_2/H_2O. The flux here represents the number of times that one reaction happens during the studied time period. These extracted mechanisms are in good agreement with previous experimental results under similar conditions [2,34–37]. Table 2 displays a reduced list of reactions which has more than 50 accumulated total flux for ethanol oxidation. Finally, there are 17 and 30 reactions remaining for O_2/N_2 and O_2/H_2O, respectively. Time evolution of some relevant key species is also shown in

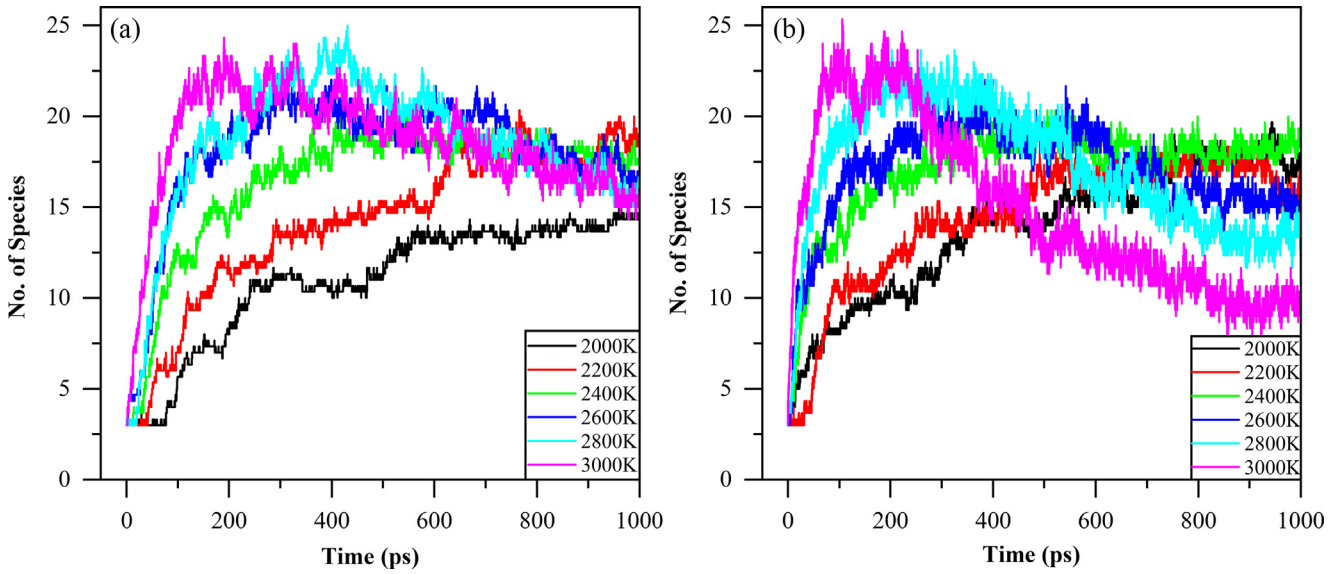

Fig. 3. Time evolution of species number during NVT MD simulations of ethanol oxidation from 2000 K to 3000 K in (a) O_2/N_2 and (b) O_2/H_2O environments.

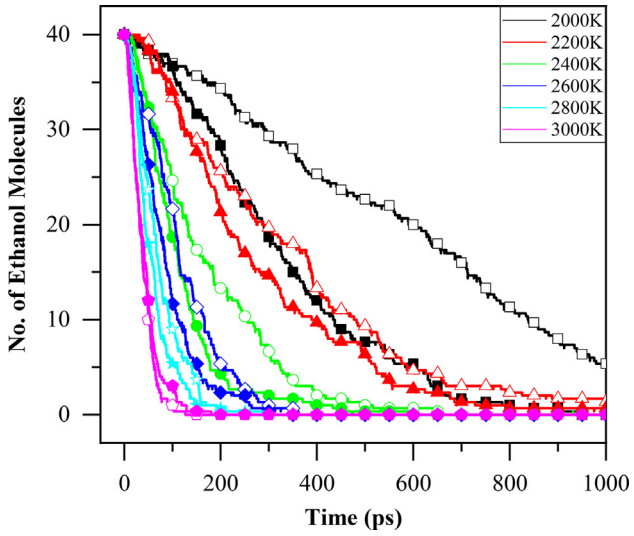

Fig. 4. Time evolution of ethanol molecule number during NVT MD simulations of ethanol oxidation with high (hollow symbol) and low (solid symbol) water content from 2000 K to 3000 K in O_2/H_2O environment.

Fig. 5.

Supplementary data associated with this article can be found, in the online version, at https://doi.org/10.1016/j.fuel.2018.08.040.

According to the extracted mechanisms, as expected, ethanol oxidation is initiated by the decomposition of ethanol forming C_2H_5 radicals, until CHO and CO radicals are seen at a very late stage. Additionally, key intermediate products such as C_2H_4, CH_3 and CH_2O are found in the reactions as well. The accordance with previous experimental results [2,34–37] proves the effectiveness and accuracy of the present ReaxFF MD method to study the reaction mechanism of ethanol oxidation. More specifically, all reactions shown in Table 2a are covered by the previous detailed kinetics studies of ethanol oxidation from Marinov [35] and Norton & Dryer [36] except a couple of minor differences. For example, R14a shows the reaction of $CH_3 + O_2 \rightarrow CH_3O_2$ instead of $CH_3 + O_2 \rightarrow CH_3O + O$, which appears in the both aforementioned two studies. But the $CH_3O_2 \rightarrow CH_3O + O$ reaction can be found in the present mechanism if a lower total flux filter is used. All the reactions displayed in Table 2 are obtained by setting certain conditions within the simulation time scale (not totally completed ethanol oxidation). Therefore, compared to some previous studies having hundreds of elementary reactions, this study focuses more on the significant differences of reaction pathways between ethanol oxidation in N_2 and H_2O environments.

3.3.1. *Chemical effects of water addition*

The different reactions within the two pathways are marked with asterisk in Table 2. As can be seen, the main discrepancies are the way of producing OH radicals and consuming the main intermediates. Fig. 5 depicts that the OH production is always higher in O_2/H_2O than in O_2/N_2. Previous experiments have proved that water addition into ethanol can promote the OH production due to the chemical effect of H_2O thereby accelerating the oxidation reactions [5,6]. Due to the high content of water, O_2/H_2O system is able to generate a large amount of OH radicals also by several other different reactions involving H_2O molecules (R3b, R4b and R5b), whereas the main sources of OH radicals in O_2/N_2 are only HO_2 and H_2O_2. Moreover, the reaction $H_2O_2 \rightarrow OH + OH$ happens much less frequently in O_2/N_2 than in O_2/H_2O. Comparing R3a with R3b, H_2O promotes the reaction of HO_2 producing OH and H_2O_2 as well, which is the main reason for the more frequently happened reaction $H_2O_2 \rightarrow OH + OH$ in O_2/H_2O. This can also explain that the level of HO_2 produced is lower and the maximum number of H_2O_2 created is more in O_2/H_2O as shown in Fig. 5. In contrast, HO_2 in O_2/N_2 has a high possibility consuming the OH radicals by reaction R4a and consequently decreases the reactivity of OH with other intermediates. This HO_2/OH mechanism combined with R4a and R9b accounts for the experimental fact that the reaction $HO_2 + OH \rightarrow H_2O + O_2$ is suppressed while the reaction $H + OH \rightarrow H_2O$ is promoted with the presence of water in ethanol [6]. As a main source of OH formation in O_2/N_2, H_2O_2 in O_2/H_2O also reacts with HO_2 and H (R7b and R8b) which further enhance the OH generation. It is worth mentioning that high water concentration contributes to increased H_2 production (displayed in Fig. 5), primarily by reaction R4b.

As discussed above, the other significant difference between the two mechanisms lies in how they consume the main intermediates. Based on Table 2, for the O_2/N_2 system, there are 3 and 4 events for C_1 & C_2 intermediates reaction with O_2 and OH, respectively, whereas the number count for O_2/H_2O system is 3 and 10. The large number of reaction events involving OH indicates that the C_1 & C_2 intermediate products favour the reaction pathway of $C_xH_yO_z + OH \rightarrow C_xH_{y-1}O_z + H_2O$ (situations are different for reactions R21b, R26b and R29b, where there is no H_2O generated) in O_2/H_2O due to the high level of OH production. Besides, reactions R14b, R17b, R23b show that

Table 2
Reduced list of elementary reactions during NVT MD simulations of ethanol oxidation in (a) O_2/N_2 and (b) O_2/H_2O environments. Different reactions within the two pathways are marked with asterisk.

ID	(a) Reaction (O_2/N_2)	Total Flux
1	$C_2H_6O \rightarrow C_2H_5 + OH$	110
2	$H + O_2 \rightarrow HO_2$	222
3	$^*HO_2 \rightarrow OH + O$	61
4	$^*HO_2 + OH \rightarrow H_2O + O_2$	110
5	$H_2O_2 \rightarrow OH + OH$	99
6	$C_2H_6O + OH \rightarrow C_2H_5O + H_2O$	179
7	$^*C_2H_6O + HO_2 \rightarrow C_2H_5O + H_2O_2$	74
8	$C_2H_5O \rightarrow C_2H_4 + OH$	82
9	$C_2H_5O \rightarrow CH_2O + CH_3$	149
10	$^*C_2H_5 + O_2 \rightarrow C_2H_4 + HO_2$	66
11	$C_2H_4 + OH \rightarrow C_2H_3 + H_2O$	63
12	$CH_3O \rightarrow CH_2O + H$	56
13	$CH_3 + OH \rightarrow CH_4O$	61
14	$^*CH_3 + O_2 \rightarrow CH_3O_2$	56
15	$CH_2O + OH \rightarrow CHO + H_2O$	96
16	$CHO \rightarrow CO + H$	57
17	$CHO + O_2 \rightarrow CO + HO_2$	68
ID	(b) Reaction (O_2/H_2O)	Total Flux
1	$C_2H_6O \rightarrow C_2H_5 + OH$	96
2	$H + O_2 \rightarrow HO_2$	301
3	$^*H_2O + HO_2 \rightarrow H_2O_2 + OH$	468
4	$^*H_2O + H \rightarrow H_2 + OH$	209
5	$^*H_2O + O \rightarrow OH + OH$	95
6	$H_2O_2 \rightarrow OH + OH$	302
7	$^*H_2O_2 + HO_2 \rightarrow H_2O + O_2 + OH$	79
8	$^*H_2O_2 + H \rightarrow H_2O + OH$	77
9	$^*H + OH \rightarrow H_2O$	81
10	$C_2H_6O + OH \rightarrow C_2H_5O + H_2O$	320
11	$^*C_2H_6O + OH \rightarrow CH_2O + CH_3 + H_2O$	60
12	$C_2H_5O \rightarrow C_2H_4 + OH$	98
13	$C_2H_5O \rightarrow CH_2O + CH_3$	171
14	$^*C_2H_5O \rightarrow C_2H_4O + H$	51
15	$^*C_2H_4O + OH \rightarrow C_2H_3O + H_2O$	62
16	$C_2H_4 + OH \rightarrow C_2H_3 + H_2O$	118
17	$^*C_2H_3O \rightarrow C_2H_2O + H$	60
18	$^*C_2H_2O + OH \rightarrow C_2HO + H_2O$	61
19	$^*CH_4O + OH \rightarrow CH_3O + H_2O$	66
20	$CH_3O \rightarrow CH_2O + H$	54
21	$CH_3 + OH \rightarrow CH_4O$	128
22	$CH_2O + OH \rightarrow CHO + H_2O$	219
23	$^*CHO_2 \rightarrow CO_2 + H$	159
24	$^*CHO_2 + O_2 \rightarrow CO_2 + HO_2$	56
25	$CHO \rightarrow CO + H$	92
26	$^*CHO + OH \rightarrow CH_2O_2$	81
27	$CHO + O_2 \rightarrow CO + HO_2$	86
28	$^*CO_3 \rightarrow CO_2 + O$	53
29	$^*CO + OH \rightarrow CHO_2$	98
30	$^*CO + O_2 \rightarrow CO_3$	61

the presence of a large amount of water advances the dehydrogenation of C_1 & C_2 intermediates via the reaction pathway of $C_xH_yO \rightarrow C_xH_{y-1}O + H$ and these 3 reactions are not seen in the reduced O_2/N_2 mechanism. The generated H radicals either directly react with OH to form H_2O (reaction R9b) or participate in the OH production related events (reactions R2b, R4b and R8b) to create more OH radicals.

3.3.2. CO and CO_2 production

As shown in Fig. 5, the number of CO molecules is always greater than CO_2 in O_2/N_2 during the simulation time, while at a late stage from 2400 K in O_2/H_2O, the number of CO_2 molecules becomes larger than CO and this turning point occurs earlier as the temperature goes up. This phenomenon cannot be seen at the low temperatures of 2000 K and 2200 K because the simulation time is not long enough to allow the reaction to proceed to that stage. Similarly, it is apparent that the number of CO molecules in O_2/H_2O has reached its maximum value and started to decrease within the simulation time at the high

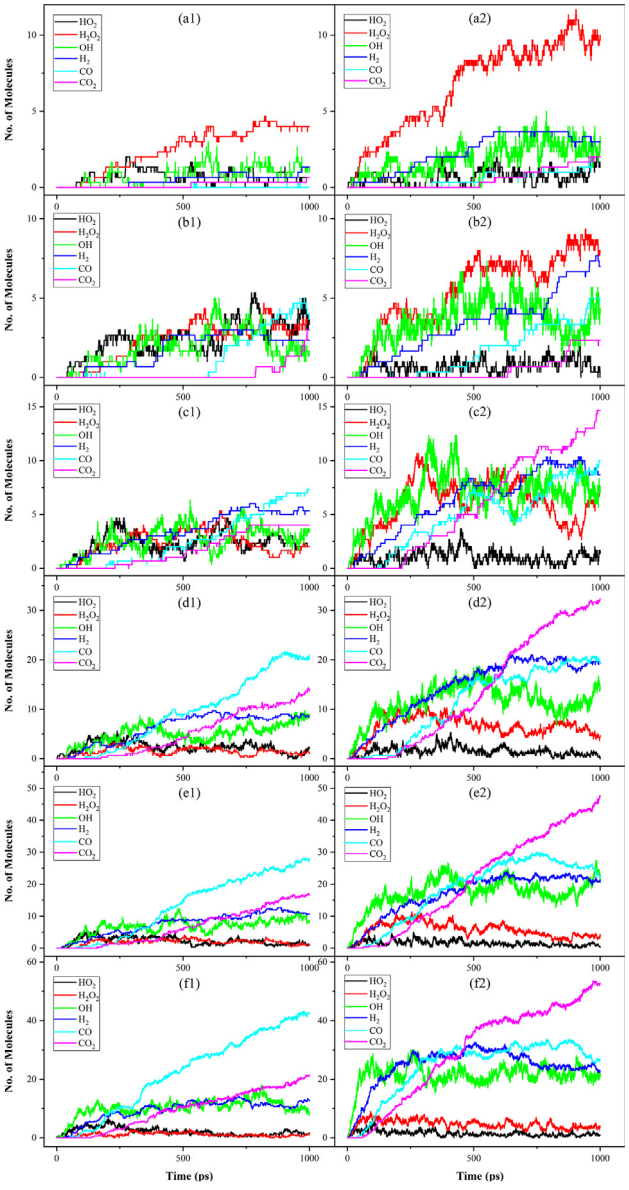

Fig. 5. Time evolution of some key species during NVT MD simulations of ethanol oxidation from 2000 K to 3000 K in (a1 ~ f1) O_2/N_2 and (a2 ~ f2) O_2/H_2O environments.

temperatures of 2800 K and 3000 K. Furthermore, the maximum number of CO produced is lower in O_2/H_2O than in O_2/N_2 and the CO number in O_2/N_2 is still increasing which has not reached its peak value at the end of the simulation. This elucidates why the number of CO molecules is close or even slightly more in O_2/H_2O than in O_2/N_2 at the temperatures below 2800 K. It is because of the faster CO production rate at the initial stage of the O_2/H_2O simulation and the insufficient simulation time for O_2/N_2. Therefore, it is believed that the number of CO molecules generated is less in O_2/H_2O than O_2/N_2 provided that the simulation time is long enough to witness both of their peaks, and CO production is therefore reduced with the presence of high content water. This outcome agrees well with the previous experimental results [6,10].

The above results can also be interpreted by the two different mechanisms. In the full list of O_2/N_2 reaction pathways, it can be seen that CO firstly reacts with O_2 to form unstable CO_3 and then decomposes to CO_2 and O (reactions R23a and R22a in Table S1). Apart from this same pathway, CO in O_2/H_2O has an alternative way to be transformed into CO_2, where OH is involved. CHO_2 is formed by the reaction of CO with

OH (reaction R29b). Afterwards, CHO_2 can either directly decompose to CO_2 and H (reaction R23b) or be oxidized by O_2 producing CO_2 and HO_2 (reaction R24b). Hence, the CO/CO_2 ratio is decreased in O_2/H_2O by converting CO to CO_2 via the aforementioned pathways so that CO_2 production is significantly higher in O_2/H_2O than in O_2/N_2 as presented in Fig. 5. Similar $CO/OH/CO_2$ pathways were also obtained from the experiment of hydrous ethanol oxidation [6]. Once again, it is the high water concentration that promotes the OH generation and then advance the conversion of CO to CO_2. On the whole, the CO production is reduced.

4. Conclusions

A series of ReaxFF MD simulations are performed to investigate the fundamental reaction mechanisms of hydrous ethanol oxidation in comparison with ethanol oxidation under fuel-air conditions. The reaction rates and detailed reaction pathways are obtained to scrutinize the effect of water addition on ethanol oxidation. The time evolution of potential energy shows that the heat absorption and release are much more and faster in O_2/H_2O than in O_2/N_2 environment. This implies that water does participate in and facilitate the reaction of ethanol oxidation. The results are further confirmed by the higher reaction rate of ethanol oxidation with water addition at all studied temperatures. According to the time evolution of species number, the presence of water advances the ionisation process and accelerates the radical production rate thereby enhancing ethanol oxidation. Two different ethanol/water ratio cases are also compared and it is suggested that water content plays a vital role in the reactions at low temperatures but that effect can be ignored at high temperatures. A new insight into water effect on ethanol oxidation is provided via the detailed reaction pathways and time evolution of relevant key species. It is determined that the main discrepancies between the two pathways lie in the way of producing OH radicals and consuming the main intermediates, which are not revealed previously. In water environment, H_2O is able to promote the reaction of some important species like HO_2, H and O as well as the associated reactions involving H_2O_2 indirectly producing a large amount of OH radicals because of the high water content whereas the main sources of OH formation in nitrogen environment are only the decomposition of HO_2 and H_2O_2. Additionally, the high level of OH production in water environment also advances its reactions with C_1 & C_2 intermediates. Furthermore, dehydrogenation of C_1 & C_2 intermediates is improved with the presence of water. Finally, the CO production is reduced in hydrous ethanol oxidation as a result of the reaction of CO with OH converting CO to CO_2 ultimately, which is not seen in O_2/N_2 mechanism. Therefore, it is the addition of water that promotes the OH production due to the chemical effect of H_2O leading to the enhancement of ethanol oxidation and reduction of CO production. This research demonstrates the feasibility and usefulness of ReaxFF-based reactive MD simulations for detailed investigation of reaction mechanisms of realistic fuel systems. It also reaffirms the scientific foundation for the direct use of hydrous ethanol as a fuel for combustion systems with a low cost.

Acknowledgements

Funding from the UK Engineering and Physical Sciences Research Council under the projects “UK Consortium on Mesoscale Engineering Sciences (UKCOMES, UK)” (Grant Nos. EP/L00030X/1 and EP/R029598/1) and “High Performance Computing Support for United Kingdom Consortium on Turbulent Reacting Flow (UKCTRF, UK)” (Grant No. EP/K024876/1) is gratefully acknowledged. The first author is also grateful for the Graduate Research Scholarship and Overseas Research Scholarship from University College London.

References

[1] Geng P, Cao EM, Tan QM, Wei LJ. Effects of alternative fuels on the combustion characteristics and emission products from diesel engines: a review. Renewable Sustainable Energy Rev 2017;71:523–34.
[2] Aghsaee M, Nativel D, Bozkurt M, Fikri M, Chaumeix N, Schulz C. Experimental study of the kinetics of ethanol pyrolysis and oxidation behind reflected shock waves and in laminar flames. Proc Combust Inst 2015;35:393–400.
[3] Onuki S, Koziel JA, van Leeuwen J, Jenks WS, Grewell DA, Cai L. Ethanol production, purification, and analysis techniques: a review. In: ASABE Annual International Meeting. Providence, RI; 2008. p. 7210–21.
[4] Martinez-Frias J, Aceves SM, Flowers DL. Improving ethanol life cycle energy efficiency by direct utilization of wet ethanol in HCCI engines. J Energy Resour ASME 2007;129(4):332–7.
[5] Rahman KM, Kawahara N, Tsuboi K, Tomita E. Combustion characteristics of wet ethanol ignited using a focused Q-switched Nd:YAG nanosecond laser. Fuel 2016;165:331–40.
[6] Liang JJ, Li GS, Zhang ZH, Xiong Z, Dong F, Yang R. Experimental and numerical studies on laminar premixed flames of ethanol-water-air mixtures. Energy Fuel 2014;28(7):4754–61.
[7] Breaux BB, Acharya S. The effect of elevated water content on swirl-stabilized ethanol/air flames. Fuel 2013;105:90–102.
[8] Saxena S, Schneider S, Aceves S, Dibble R. Wet ethanol in HCCI engines with exhaust heat recovery to improve the energy balance of ethanol fuels. Appl Energy 2012;98:448–57.
[9] Mack JH, Aceves SM, Dibble RW. Demonstrating direct use of wet ethanol in a homogeneous charge compression ignition (HCCI) engine. Energy 2009;34(6):782–7.
[10] Munsin R, Laoonual Y, Jugjai S, Imai Y. An experimental study on performance and emissions of a small SI engine generator set fuelled by hydrous ethanol with high water contents up to 40%. Fuel 2013;106:586–92.
[11] Ambros WM, Lanzanova TDM, Fagundez JLS, Sari RL, Pinheiro DK, Martins MES, et al. Experimental analysis and modeling of internal combustion engine operating with wet ethanol. Fuel 2015;158:270–8.
[12] Lanzanova TDM, Dalla Nora M, Zhao H. Performance and economic analysis of a direct injection spark ignition engine fueled with wet ethanol. Appl Energy 2016;169:230–9.
[13] Costa RC, Sodre JR. Hydrous ethanol vs. gasoline-ethanol blend: engine performance and emissions. Fuel 2010;89(2):287–93.
[14] Masum BM, Masjuki HH, Kalam MA, Fattah IMR, Palash SM, Abedin MJ. Effect of ethanol-gasoline blend on NOx emission in SI engine. Renewable Sustainable Energy Rev 2013;24:209–22.
[15] van Duin ACT, Dasgupta S, Lorant F, Goddard WA. ReaxFF: a reactive force field for hydrocarbons. J Phys Chem A 2001;105(41):9396–409.
[16] Chenoweth K, van Duin ACT, Goddard 3rd. WA. ReaxFF reactive force field for molecular dynamics simulations of hydrocarbon oxidation. J Phys Chem A 2008;112(5):1040–53.
[17] Russo MF, van Duin ACT. Atomistic-scale simulations of chemical reactions: bridging from quantum chemistry to engineering. Nucl Instrum Meth B 2011;269(14):1549–54.
[18] Senftle TP, Hong S, Islam MM, Kylasa SB, Zheng Y, Shin YK, et al. The ReaxFF reactive force-field: development, applications and future directions. npj Comput Mater 2016;2:15011.
[19] Aktulga HM, Fogarty JC, Pandit SA, Grama AY. Parallel reactive molecular dynamics:numerical methods and algorithmic techniques. Parallel Comput 2012;38(4):245–59.
[20] Plimpton S. Fast parallel algorithms for short-range molecular dynamics. J Comput Phys 1995;117(1):1–19.
[21] Hong D, Guo X. A reactive molecular dynamics study of CH4 combustion in O2/CO2/H2O environments. Fuel Process Technol 2017;167:416–24.
[22] Feng M, Jiang XZ, Luo KH. A reactive molecular dynamics simulation study of methane oxidation assisted by platinum/graphene-based catalysts. Proc Combust Inst 2018. https://doi.org/10.1016/j.proci.2018.05.109.
[23] Bhoi S, Banerjee T, Mohanty K. Molecular dynamic simulation of spontaneous combustion and pyrolysis of brown coal using ReaxFF. Fuel 2014;136:326–33.
[24] Castro-Marcano F, Kamat AM, Russo MF, van Duin ACT, Mathews JP. Combustion of an Illinois No. 6 coal char simulated using an atomistic char representation and the ReaxFF reactive force field. Combust Flame 2012;159(3):1272–85.
[25] Chenoweth K, van Duin ACT, Dasgupta S, Goddard WA. initiation mechanisms and kinetics of pyrolysis and combustion of JP-10 hydrocarbon jet fuel. J Phys Chem A 2009;113(9):1740–6.
[26] Mao Q, van Duin ACT, Luo KH. Investigation of methane oxidation by palladium-based catalyst via ReaxFF molecular dynamics simulation. Proc Combust Inst 2017;36(3):4339–46.
[27] Dontgen M, Przybylski-Freund MD, Kroger LC, Kopp WA, Ismail AE, Leonhard K. Automated discovery of reaction pathways, rate constants, and transition states using reactive molecular dynamics simulations. J Chem Theory Comput 2015;11(6):2517–24.
[28] Jiang XZ, Feng M, Zeng W, Luo KH. Study of mechanisms for electric field effects on ethanol oxidation via reactive force field molecular dynamics. Proc Combust Inst 2018. https://doi.org/10.1016/j.proci.2018.07.053.
[29] Hong DK, Liu L, Huang Y, Zheng CG, Guo X. Chemical effect of H2O on CH4 oxidation during combustion in O-2/H2O environments. Energy Fuel 2016;30(10):8491–8.
[30] Liu LC, Bai C, Sun H, Goddard WA. Mechanism and kinetics for the initial steps of

pyrolysis and combustion of 1,6-dicyclopropane-2,4-hexyne from ReaxFF reactive dynamics. J Phys Chem A 2011;115(19):4941–50.
[31] Wang HJ, Feng YH, Zhang XX, Lin W, Zhao YL. Study of coal hydropyrolysis and desulfurization by ReaxFF molecular dynamics simulation. Fuel 2015;145:241–8.
[32] Mao Q, van Duin ACT, Luo KH. Formation of incipient soot particles from polycyclic aromatic hydrocarbons: a ReaxFF molecular dynamics study. Carbon 2017;121:380–8.
[33] Humphrey W, Dalke A, Schulten K. VMD: Visual molecular dynamics. J Mol Graph Model 1996;14(1):33–8.
[34] Cancino LR, Fikri M, Oliveira AAM, Schulz C. Measurement and chemical kinetics modeling of shock-induced ignition of ethanol-air mixtures. Energy Fuel 2010;24(5):2830–40.
[35] Marinov NM. A detailed chemical kinetic model for high temperature ethanol oxidation. Int J Chem Kinet 1999;31(3):183–220.
[36] Norton TS, Dryer FL. An experimental and modeling study of ethanol oxidation-kinetics in an atmospheric-pressure flow reactor. Int J Chem Kinet 1992;24(4):319–44.
[37] Saxena P, Williams FA. Numerical and experimental studies of ethanol flames. Proc Combust Inst 2007;31:1149–56.